Interdecadal-Decadal Climate Variability from Multi-Coral Oxygen Isotope Records in the South Pacific Convergence Zone Region Since 1650 A.D.

Braddock K. Linsley*+; Department of Earth and Atmospheric Sciences, University at Albany, State University of New York, Albany, New York, USA (phone: 518-442-4478), (blinsley@albany.edu)

Peipei Zhang+; Department of Earth and Atmospheric Sciences, University at Albany, State University of New York, Albany, New York, USA (zhang_pei_pei@hotmail.com)

Alexey Kaplan; Lamont-Doherty Earth Observatory of Columbia University, Palisades, New York, USA (alexeyk@ldeo.columbia.edu)

Stephen S. Howe; Department of Earth and Atmospheric Sciences, University at Albany, State University of New York, Albany, New York, USA (showe@albany.edu)

Gerard M. Wellington; Department of Biology, University of Houston, Houston, Texas, USA

* = corresponding author
+= these authors contributed equally to this work

Submitted to Paleoceanography: September 5, 2007
Minor Revisions submitted: February 28, 2008
Final Acceptance: March 12, 2008

Index terms:

Coral $\delta^{18}O$, Interdecadal-decadal climate variability, Paleoclimatology, SPCZ, WPWP

ABSTRACT

In the South Pacific, interdecadal-decadal oceanic and atmospheric variability, referred to as the Interdecadal Pacific Oscillation (IPO), is most pronounced in the South Pacific Convergence Zone (SPCZ) salinity front region. Here we have used annual average oxygen isotope ($\delta^{18}O$) time series from five coral cores collected from Fiji and Tonga in this region to construct a Fiji-Tonga Interdecadal-Decadal Pacific Oscillation (F-T IDPO) index of low frequency (>9yr and <55yr) climate variability back to 1650 A.D. We first demonstrate the consistency between this F-T IDPO index and a mean sea level (MSL) pressure-based SPCZ Position Index (SPI) (1891-2000), thus verifying the ability of coral $\delta^{18}O$ to record past interdecadal-decadal climatic variations in this region back to 1891. The F-T IDPO index is then shown to be synchronous with the IPO index (1856-2000), suggesting that this coral-based index effectively represents the interdecadal-decadal scale climate variance back to 1650. The regularity of the F-T IDPO Index indicates that interdecadal-decadal variability in the SPCZ region has been relatively constant over the past 350 years with a mean frequency of ~20 years (variance peaks near 11 and 35yrs). There is a consistent anti-phase correlation of the F-T IDPO index and the interdecadal-decadal components in equatorial Pacific coral $\delta^{18}O$ series from Maiana and Palmyra. This observation indicates that the eastward expansion (westward contraction) of the eastern salinity front of the Western Pacific Warm Pool (WPWP) occurs simultaneously (± <1yr) with the westward (eastward) shift of the SPCZ salinity front during positive IPO (negative IPO) phases. This is the same relationship

observed during the phases of the El Niño Southern Oscillation.

1. Introduction

The South Pacific Convergence Zone (SPCZ) is a reverse-oriented monsoonal low-pressure trough stretching from the Intertropical Convergence Zone (ITCZ) near the Solomon Islands to Fiji, Samoa, Tonga and farther southeast to French Polynesia (Figure 1). This region features a large sea surface temperature (SST) gradient and active low-level convergence. The low-level convergence of moisture leads to a persistent cloud band as well as showers and thunderstorms. Precipitation and convection within the band is seasonally dependent. Its equatorial portion, where it is connected to the ITCZ, is most active in the Southern Hemisphere summer, and the more southeasterly portion is most active during transition seasons of fall and spring. On interannual timescales, displacements of the SPCZ are relatively well known. During La Niña phases the SPCZ shifts southwestward and during El Niño phases the SPCZ shifts northeast toward Samoa [*Folland et al.*, 2002; *Gouriou and Delcroix,* 2002]. However, lower-frequency displacements are less well understood due to the lack of long-term instrumental records. *Folland et al.* [2002] have developed a SPCZ position index (SPI) from the monthly instrumental mean sea level (MSL) pressure differences between Suva, Fiji (18°9'S, 178°26'E) and Apia, Samoa (13°48'S, 171°47'W) from November to April during the period 1891-2000 (see Figure 2). The SPI was found to be closely correlated with the phase of the Interdecadal Pacific Oscillation (IPO), with

the SPCZ displaced towards Fiji during negative phases of the IPO and towards Samoa during positive phases of the IPO [*Folland et al.,* 2002]. At lower frequencies, *Linsley et al.* [2006] have interpreted the secular trends in replicated coral oxygen isotope ($\delta^{18}O$) records from Fiji and Rarotonga as evidence that the SPCZ has been expanding southeast since the mid 1800s.

At the southeastern edge of the SPCZ, oceanic circulation around the feature in conjunction with a positive precipitation-evaporation (P-E) balance in the SPCZ creates a salinity gradient in the ocean, with fresher and warmer waters of the western Pacific lying to the west of the salinity front and cooler, saltier waters lying to the east [*Gouriou and Delcroix,* 2002](see Figures 1 and 2). On interannual scales, when the SPCZ migrates northeastward (southwestward) during El Niño (La Niña) events, the salinity front simultaneously shifts northwestward (southeastward) [*Gouriou and Delcroix,* 2002; *Juillet-Leclerc et al.,* 2006; *Linsley et al.,* 2006]. On interdecadal time-scales the SPCZ salinity front also migrates northwestward (southeastward) during the negative (positive) phase of the Interdecadal Pacific Oscillation (IPO) (see Figure 1), e.g., westward during the late 1940s to mid 1970s and eastward after the mid 1970s [*Delcroix et al.,* 2007].

In many studies, $\delta^{18}O$ series in corals have been shown to provide a unique record of past climatic variability due to: 1) the precise dating provided by annual growth bands combined with $\delta^{18}O$ annual cycles and 2) the ability of coral skeletal $\delta^{18}O$ to record environmental changes [e.g., *Wellington et al.,* 1996]. However, limitations of

using the coral $\delta^{18}O$ proxy include uncertainties both in the combined effects of SST and the $\delta^{18}O$ of seawater and in the effects of poorly understood potential biological artifacts such as inconsistent annual skeletal extension rates and calcification rates [*Lough, 2004*]. Skeletal diagenesis either via secondary calcification or dissolution can also be hard to detect [*Mueller et al., 2001; Hendy et al., 2007*].

Here we use a regional multi-coral $\delta^{18}O$ series approach in an attempt to minimize potential biological or diagenetic artifacts and to increase the climate signal to noise ratio of the interdecadal-decadal $\delta^{18}O$ variability. The climatic significance of interdecadal-decadal modes in coral $\delta^{18}O$ time-series is still under debate [e.g., *Jones et al.,* 1998; *Crowley et al.,* 1999; *Evans et al.,* 2000; *Linsley et al.,* 2004, 2006]. To examine the reliability of the coral-based $\delta^{18}O$ proxy in reconstructing interdecadal and decadal climate variability in the past, we isolated the interdecadal-decadal modes in five coral $\delta^{18}O$ time-series in the SPCZ region (two from Fiji and three from Tonga) (Figure 2). Both island chains lie in an area of the South Pacific where the IPO is most pronounced (see Figure 1). *Folland et al.* [2002] demonstrated the equivalence of the IPO and the North Pacific derived Pacific Decadal Oscillation (PDO) index. In the South Pacific the IPO amplitude appears to be of similar magnitude to the El Niño Southern Oscillation (ENSO). Large uncertainties remain regarding the temporal and spatial coherence of this interdecadal-decadal variability prior to ~1950 when instrumental data were less complete in coverage and are generally thought to be less reliable. Here we will show that the interdecadal-decadal variability extracted from the $\delta^{18}O$ series of five corals

from Fiji and Tonga correlates with the SPI and IPO indices. This demonstrates the reliability of coral $\delta^{18}O$ from Fiji and Tonga as a climate proxy at interdecadal-decadal frequencies and establishes that a five-coral $\delta^{18}O$ composite Interdecadal-Decadal Pacific Oscillation (IDPO) Index back to 1650 A.D. documents past interdecadal-decadal climate oscillations.

2. Methods

2.1 Sampling and Chronology

In November 2004 three *Porites lutea* coral colonies were drilled at Tonga on the islands of Ha'afera, Malinoa and Nomuka Iki (Figure 2). At Ha'afera (19°56'S, 174°43'W), a large colony with a dead flat top but with live sides was cored (see Table 1). The colony was ~4 m high with ~1 m of water covering the top at low tide. Two coral cores TH1 Hole 4 (TH1-H4 hereafter) and TH1 Hole 5 (TH1-H5 hereafter) were collected from this colony. The 3.28-m -long core TH1-H4 was drilled from the dead top of the colony and the 67-cm-long core TH1-H5 was collected from the live side of the colony. As discussed below, TH1-H4 and TH1-H5 were spliced together using the timing of known El Niño events. At Malinoa (21°02'S, 175°08'W), just north of Nuku'alofa in southern-most Tonga, a 1.63-m-long core (TM1) was collected from a living colony in 6 m of water. At Nomuka Iki (20°16'S; 174°49'W) two useable cores were collected from a large living colony in 3.5 m of water (TNI2-H1, 4.03m useable length; and TNI2-H3, 1.8m useable length). Due to a bio-eroded zone from ~1m to

130 1.68m in TNI2-H1, TNI2-H3 was drilled to allow sampling around the bio-eroded zone
131 by splicing the $\delta^{18}O$ record from H3 onto H1.

132 The $\delta^{18}O$ data from the two Fiji *Porites lutea* cores (Fiji 1F and Fiji AB) used in
133 this study were originally discussed in *Linsley et al.* [2004, 2006]. It should be noted
134 that subsequent to publishing the Fiji core AB chronology in *Linsley et al.* [2006], we
135 determined that a 2-year gap existed in this core (missing years 1727 and 1728) at a
136 core break. For this current work we have inserted two years by calculating the average
137 of each decade on either side of the gap. *Bagnato et al*. [2004] evaluated the variability
138 in a $\delta^{18}O$ time-series (2001-1776 A.D.) generated from a *Diploastrea* coral core
139 collected in the same bay as Fiji cores 1F and AB. *Diploastrea* skeletons extend at a
140 rate that is 2-3 times slower than *Porites* in the same setting. Given the possible
141 biological effects of this slower growth on skeletal geochemistry [*Pätzold,* 1984;
142 *Bagnato et al.*, 2004] we have elected not to include this *Diploastrea* time-series in our
143 *Porites* $\delta^{18}O$ composite. In addition, if any non-climatic (biological and/or digenetic)
144 effects on skeletal $\delta^{18}O$ in each coral record used in the composite are independent and
145 not related to each other, this non-climatic signal will be minimized or canceled out by
146 averaging multiple coral records, assuming the climatic signal preserved is the same for
147 all corals used in the average. Since, in slow-growing corals like *Diploastrea*, the
148 climatic vs. non-climatic components are not as well understood as they are in *Porites*,
149 we decided not to include cores of any species of coral other than *Porites lutea.*

150 All of the Tonga coral cores were cut into ~7-mm-thick slabs in the laboratory with

151 a modified tile saw, cleaned and air-dried. The slabs were X-rayed (35kV for 90
152 seconds) to reveal the density bands. All of the Tonga coral slabs were then cleaned
153 with a high-energy (500W, 20kHz) probe sonicator in a deionized water bath for
154 approximately 6 minutes and air-dried. As previously described [*Linsley et al.,* 2004,
155 2006] the Fiji coral core 1F and AB slabs were cut to a thickness of 6 mm and then
156 cleaned in a 160W ultrasonic bath prior to sampling and analysis. Dry slabs were
157 sampled using a low-speed micro-drill with a 1-mm-diameter diamond drill bit parallel
158 to corallite traces along growth axes (as identified in the X-radiographs). Each Tonga
159 core was sampled at 1-mm intervals through the top ~30 years, by excavating a
160 4-5-mm-wide (perpendicular to the growth axis) and 2-3-mm-deep groove in the coral
161 slabs. Below the top ~30 years of growth in the Tonga cores a technique of annual-scale
162 sampling was used (described below). In order to sample continuously along the growth
163 axes, the sampling track was purposely shifted from one growing axis to another as
164 sampling progressed downcore. Shifting the sampling track was also necessary to
165 bypass possible gaps caused by irregular core breaks (see example X-ray collage in
166 supplemental Figure 1). In these cases, all of the shifts were made along a distinct
167 density band to avoid any temporal hiatus in our data. The Fiji cores were sampled at
168 1-mm intervals from the top to the bottom of each core.

169 Approximately 100 μg of coral powder in each sample was dissolved in 100%
170 H_3PO_4 at 90°C in a MultiPrep sample preparation device and the generated CO_2 gas was
171 analyzed by a Micromass Optima gas-source triple-collector mass spectrometer at the

University at Albany, State University of New York Stable Isotope Ratio Mass Spectrometry Laboratory. Table 2 lists the number of samples analyzed from each Tonga core, the average difference between replicate samples and the average difference of the NBS-19 standards run by week. Approximately 13% of the 3,300 Tonga coral samples were analyzed in duplicate. All data are expressed in the conventional delta notation as per mil deviations relative to Vienna Peedee Belemnite (VPDB).

For the most recent three decades of cores TH1-H4, TH1-H5, TM1, and TNI2-H3, the chronologies are based on the reconstructed annual cycles in millimeter-scale $\delta^{13}C$ and $\delta^{18}O$ data with the warmest time set as March. The 1974-1975 La Niña, 1971-1972 La Niña，1964-1965 El Niño, and 1955-1957 La Niña events were set as control points to determine the age of TH1-H4 (the same colony as TH1-H5, but dead on the top). La Niña events result in warmer and lower salinity conditions in Fiji and Tonga (opposite from the equatorial Pacific) that lower coral $\delta^{18}O$, while during El Niño phases, locally cooler and saltier conditions result in higher coral $\delta^{18}O$ values. Figure 3 shows the mm-scale $\delta^{18}O$ results from cores TH1-H4, TH1-H5 and TNI2-H3 to illustrate the match of the interannual $\delta^{18}O$ changes with known ENSO events. We added TH1-H5 on top of TH1-H4 (the overlapping part was averaged) and named the combined time series dataset spanning 1794-2004 TH1.

Below the millimeter-scale sampling, we have utilized an annual-average sampling method, which is based on the annual density cycles identified by using X-ray

193 radiographs and ultraviolet light. Sampling was done along the maximum growth axis
194 as with the mm-scale sampling, but only one continuous sample was drilled through
195 each density band (~8-17 mm long, depending on the coral extension rates). Powder
196 from each annual accretion drilling was well mixed and its $\delta^{18}O$ value was taken as a
197 one-year average value of the corresponding year. Millimeter sampling was applied in
198 intervals where the density bands were not clear enough to identify the annual growth
199 increments. Unlike the millimeter-scale sampled Fiji cores (Fiji 1F [*Linsley et al.,*
200 2004] and Fiji AB [*Linsley et al.,* 2006]), whose annual average $\delta^{18}O$ values were
201 derived from all the data points between the two most negative $\delta^{18}O$ values of each year
202 (March), the annual average $\delta^{18}O$ values from the annual-scale drilling of the Tonga
203 cores are not necessarily 12-month averages. In the Tonga cores, although most of the
204 dense bands appear right before the warmest time in each year (January/February), there
205 are exceptions that cause differences in time spans of some years. Instead of an
206 integrated one-year cycle, several months could be missed and added to the year before
207 or after. However, as discussed below, the similarity of the resulting modes in different
208 frequencies among the five coral cores confirms the practical reliability of our sampling
209 technique.

210 **2.2 Statistical Analysis**

211 Following the approach of *Vautard and Ghil* [1989] and *Vautard et al.* [1992] we
212 performed Singular Spectrum Analysis (SSA) of the annually averaged coral $\delta^{18}O$
213 time-series. We used an SSA program written by E. Cook (Lamont-Doherty Earth

Observatory) for this analysis. SSA has been previously applied to coral time series [e.g.; *Dunbar et al., 1994; Linsley et al*., 1994, 2000*; Charles et al.,* 1997]. SSA is a fully nonparametric analysis technique based on principal component analysis that decomposes time series into several significant frequency components. It uses M-lagged copies of a centered time series to calculate eigenvalues and eigenvectors of their covariance matrix. The sampled time series X of length N is used to fill in a (N-M+1)$\times$ M matrix by taking as state vectors the consecutive sequences $Z_n = (X_n, X_{n+1} \ldots \quad X_{n+m-1})$ from n=1 to N-M+1. Variable M is called the embedding dimension or window width. Frequency separation increases as M increases, whereas statistical significance of correlations decreases. The value of M should not exceed N/3 [*Vautard et al.,* 1992]. Reconstructed components (RC's) are then calculated which allow a unique expansion of the signal into a sum of the different components. A detailed description of this technique and its paleoclimate application is given by *Vautard and Ghil* [1989] and *Vautard et al.* [1992].

Varying window widths were applied over a reasonable range to the annually averaged $\delta^{18}O$ time series data of each core. The stable features of the eigenvectors were evaluated and an appropriate M value was selected to resolve the IPO band (~9-55 years) which was the focus of this research. Since the time series are of different lengths, M varied between cores. The SSA results presented here are based on the following M settings: Fiji 1F with M=40 (N=216), Fiji AB with M=55 (N=384), Tonga TH1 with M=30 (N=212), TNI2 with M=50 (N=355) and TM1 with M=40 (N=168).

3. Results

An offset in mean $\delta^{18}O$ value previously observed for several other replicated coral records [*Tudhope et. al,* 1995*; Linsley et al.,* 1999, 2004, 2006; *Cobb et al.,* 2003] also exists in some of the five corals studied here. The 20th century mean values for annually averaged $\delta^{18}O$ are -4.64‰ for core AB, -5.06‰ for core 1F, -4.88‰ for core TH1, -4.70‰ for core TNI2, and -4.43‰ for core TM1. In the three Tonga corals, the offsets could be due to mean SST or sea surface salinity (SSS) differences between sites TH1, TNI2 and TM1. In the case of the two Fiji cores, the offset is 0.42‰. These *Porites* colonies are growing in the same setting at the same water depth within 200 m of each other in Savusavu Bay and this difference in mean $\delta^{18}O$ could be due to a difference in the disequilibrium $\delta^{18}O$ offset. Given the uncertainty of the significance of this offset from equilibrium $\delta^{18}O$, we have "centered" each of the five coral $\delta^{18}O$ series by subtracting the twentieth century mean $\delta^{18}O$ value of each core in order to facilitate comparison of the $\delta^{18}O$ time series. Centered $\delta^{18}O$ series for the five cores are shown in Figure 4. Since all five colonies are composed of the same species of coral and are from a relatively small area, they should contain common variance due to regional climatic variability.

Because these are annual averaged $\delta^{18}O$ time-series, we expect to see small differences between the amplitude of $\delta^{18}O$ "events" within any given year. For example, the 1982-83 El Niño event (marked by arrows on Figure 4) resulted in a

256 simultaneous increase in coral $\delta^{18}O$ values in all five corals. The difference in $\delta^{18}O$
257 amplitude of this El Niño event (and other events) in each core may be in part related to
258 uncertainties associated with measuring $\delta^{18}O$ in one-year increments. These include
259 analytical uncertainties (at least ±0.045‰, see table 2) and errors produced by the
260 inevitable mismatches between the length of the sample increment and the actual length
261 of the annual cycle (probably at least ±0.1‰ based on amplitude of SST annual cycle).
262 The total uncertainty could easily be ±0.15‰. There is also the possibility of biological
263 effects, such as short-term bleaching affecting one coral colony but not others. This may
264 be the case for the 1982-83 El Niño that resulted in a ~0.15‰ increase in $\delta^{18}O$ in the
265 Tonga cores TH1 and TNI2 and in the Fiji cores 1F and AB, but which caused an even
266 more pronounced 0.5‰ increase in $\delta^{18}O$ in Tonga core TM1.

267 Four out of the five corals show a clear, gradual trend toward warmer and fresher
268 conditions since the late 1800s (Figure 4), which probably indicates a southeastward
269 shift of SPCZ and associated SSS front [*Linsley et al.,* 2006]. The only exception is
270 TNI2 which records a less obvious trend that is partly obscured by an abrupt 0.3‰
271 decrease in $\delta^{18}O$ between 1915 and 1916. We believe this "jump" is the result of an
272 unknown biological or diagenetic effect and/or the possible tectonic shifting of water
273 depth at the coral site (the active Tonga trench is nearby), since the synchronous $\delta^{13}C$
274 values are normal and there did not exist any known climatic event that could change
275 the temperature and/or salinity to cause a 0.3‰ drop in $\delta^{18}O$.

276 We performed SSA to quantify the variance in the annual-averaged coral $\delta^{18}O$

277 time series from each core. For the coral $\delta^{18}O$ series analyzed in this study, we
278 separated the oscillatory components into three groups: trend, interdecadal-decadal, and
279 ENSO. The ENSO band was set to frequencies ranging between 3-8 years. This
280 frequency cut-off for ENSO has been widely applied and is based on the recurrence
281 interval of recent El Niño events. The SSA results for Core TH1 also show biennial
282 components that we did not include in the ENSO band. The mean frequencies of
283 interdecadal-decadal band were set between ~9 and ~55 years. Below, we will refer to
284 this band as the Interdecadal-Decadal Pacific Oscillation (IDPO). Since the IDPO actual
285 frequency in the Pacific is still under debate and has previously been defined as the
286 quasi-decadal oscillation [*Mann and Park,* 1994], the bidecadal oscillation [*Minobe et*
287 *al.,* 2002], and the PDO/IPO, we took a conservative approach and elected not to
288 subdivide this component. Thus the IDPO-band includes all oscillations with
289 frequencies lower than ENSO and higher than the secular trend. Here we defined the
290 secular trend as frequencies >75 years. We note that in the five coral $\delta^{18}O$ time series no
291 oscillatory components have mean frequencies between 55 and 75 years, thus 75 years
292 appears to be a logical frequency cutoff to separate the interdecadal variability from the
293 secular trend.

294 SSA of the Tonga and Fiji coral $\delta^{18}O$ records indicates that between 13%-38% of
295 the variance in each annual-averaged time series is in the IDPO band with mean periods
296 between ~9 and ~55 years. The percent variance of IDPO or ENSO bands varies in each

297 core with core TM1 having the most pronounced IDPO variance at 38.4%, which is
298 about twice as large as in the other cores. Besides the exceptionally large variance, the
299 IDPO of TM1 exhibits a perceptibly different amplitude pattern from the other four
300 cores. A possible explanation is that TM1 (near Nuku'alofa, in southern Tonga) lies at
301 the boundary between two climate regions [*Salinger et al.,* 1995] and is not only
302 influenced by southeast trade winds but also by southern westerlies in the anticyclonic
303 belt, while the four other corals are mainly affected by southeast trade winds. This coral
304 is also the only one to contain significant fungal pigments [*Priess et al.,* 2000].

305

306 **4. Discussion**

307 **4.1 Temperature vs. Salinity Contribution to $\delta^{18}O$ Variability**

308 Analysis of instrumental SST, sea surface salinity (SSS), and precipitation records in
309 the SPCZ - SSS front region beginning in 1976 indicate that each contains an interannual
310 signal that correlates with the Southern Oscillation Index (SOI) and ENSO [*Gouriou and*
311 *Delcroix,* 2002]. In this region the amplitudes of the interannual signals in SST and
312 precipitation are an order of magnitude less than the amplitude of the seasonal cycle,
313 whereas for SSS, the interannual signal of 1 to 1.5 p.s.u. is double the amplitude of the
314 seasonal signal [*Gouriou and Delcroix,* 2002]. At both Fiji and Tonga instrumental 2° x
315 2° latitude-longitude gridded SST [*Reynolds and Smith,* 1994] and 2° x 10°
316 latitude-longitude gridded SSS [*Gouriou and Delcroix,* 2002] records reveal that each site

317 has a pronounced seasonal SST cycle of 4° to 5°C and a weak seasonal SSS cycle. On
318 interannual time scales the opposite takes place, a weak SST signal of 1° to 2°C and a
319 larger 1 to 1.5 p.s.u. SSS signal (Figure 5).

320 Since it is known that coral skeletal $\delta^{18}O$ is primarily related to water temperature
321 and $\delta^{18}O$ of seawater, we expected to see influences of both parameters in these coral
322 $\delta^{18}O$ series. *Linsley et al.* [2006] showed that when analyzed at a resolution of ~10
323 samples per year, the Fiji coral $\delta^{18}O$ signal is strongly modulated by the 4-5°C annual
324 SST cycle, with interannual variability predominantly driven by SSS. For both Fiji and
325 Tonga the seasonal $\delta^{18}O$ range of
326 0.8 –1.0‰ is close to that expected for the 4°-5°C annual SST cycle [*Epstein et al., 1953;*
327 *Dunbar et al.,* 1994*; Wellington et al.,* 1996]. Interannual coral $\delta^{18}O$ variability appears to
328 be largely the result of the 1-1.5 p.s.u. irregular interannual SSS cycle and the advection
329 of the SSS front in response to ENSO.

330 Figure 5 compares Tonga cores TH1, TNI2, and TM1 and Fiji cores 1F and AB
331 annual-averaged $\delta^{18}O$ data to annual-averaged SSS from *Gouriou and Delcroix* [2002]
332 and annual SST anomaly from the Hadley Center Sea Ice and Sea Surface temperature
333 database (HadISST1). Correlation coefficients (r-value) between annual-averaged coral
334 $\delta^{18}O$ and SSS over the interval from 1976 to 2000 are 0.61 for Tonga core TH1, 0.52
335 for Tonga core TNI2, 0.62 for Tonga core TM1, 0.66 for Fiji core 1F and 0.71 for Fiji
336 core AB (*average 5 coral vs. SSS r-value = 0.62*). Correlation coefficients between
337 annual averaged $\delta^{18}O$ and SST during 1870 to 1996 are -0.44 for Tonga core TH1,

338 -0.46 for Tonga core TNI2, -0.41 for Tonga core TM1, -0.54 for Fiji core 1F and -0.64
339 for Fiji core AB (*average 5 coral vs. SSTa r-value =-0.50*). Assuming that the
340 relationship between coral $\delta^{18}O$ and SST is -0.21‰/°C (-0.17 to -0.23‰/°C is the
341 common range of coral $\delta^{18}O$-SST calibrations [*Epstein et al.,* 1953*; Dunbar et al.,* 1994*;*
342 *Gagan et al.,* 1994*; Wellington et al.,* 1996]), the 1°C interannual range of annual SST
343 of both Tonga and Fiji from the HadISST1 during 1976-2000 contributes ~0.21‰ to the
344 change in coral $\delta^{18}O$ in this time interval. Subtracting this 0.21‰ SST portion from the
345 total coral $\delta^{18}O$ range (~0.5‰) during the same period of time results in a residual of
346 ~0.3‰. The magnitude of the "residual" is in accord with the interannual 1-1.2 p.s.u.
347 range based on the 0.27 to 0.45‰/p.s.u. range between $\delta^{18}O_{seawater}$ and SSS found for
348 the equatorial western Pacific and South Pacific [*Fairbanks et al.,* 1997*; Morimoto et al.,*
349 2002*; LeGrande and Schmidt,* 2006]. We realize that the 0.27‰/p.s.u. relationship
350 derived from the equatorial Pacific by Fairbanks et al. [1997] may be conservative and
351 underestimate the amplitude of SSS variability for a given coral $\delta^{18}O$ change in this
352 region. In the South Pacific, a 0.45‰/p.s.u relationship was derived from limited data
353 [*LeGrande and Schmidt,* 2006]. Using this relationship the residual ~0.3‰ coral $\delta^{18}O$
354 signal would reflect a 1.5 p.s.u. SSS change which is supported by the instrumental
355 salinity data (see Figure 5).

356 ENSO event and IPO phase effects on SST and $\delta^{18}O_{seawater}$ in this region result in
357 additive effects on coral $\delta^{18}O$. For example, during El Niño events and/or positive

358 phases of the IPO index, locally cooler and saltier conditions increase coral $\delta^{18}O$ at Fiji
359 and Tonga. The opposite occurs during La Niña events or negative IPO intervals. Since
360 greater precipitation, advection of lower salinity water, and warmer temperatures (or
361 drier/saltier conditions with cooler temperatures) occur together in the study area
362 [*Folland et al.,* 2002], their effects should be additive on coral $\delta^{18}O$. Thus, we
363 interpret coral $\delta^{18}O$ variability in this region as an index of ENSO or the IPO/PDO
364 without separating the effects of SST and SSS.

365

366 **4.2 Fiji-Tonga Interdecadal-Decadal Pacific Oscillation Index**

367 Although the five coral cores were collected from a relatively small area (5°-6°
368 latitude-longitude) along the salinity front at the southeast boundary of the SPCZ, the
369 colonies grew in water of different depths in different lagoon/fore-reef settings. TH1
370 was collected in an isolated lagoon in 1 m water. TNI2 was collected from a colony in
371 3.5 m of water in a well-flushed passage. TM1 grew more slowly (~4-12 mm/yr) than
372 the other cores (~7-15 mm/yr) and contained residue pigments along the density bands
373 from fungal growth [*Priess et al.,* 2000]. Fiji Core AB [*Linsley et al.,* 2006] and Fiji
374 core 1F [*Linsley et al.,* 2004] were collected at 10 m depth within 200 m of each other in
375 Savusavu Bay.

376 Despite various biological and unknown effects in these diverse settings that could
377 potentially influence the skeletal $\delta^{18}O$, we find that once the $\delta^{18}O$ series are corrected

for differences in disequilibrium offset (as in *Linsley et al.,* 1999), the annually averaged $\delta^{18}O$ series contain common variance that can be attributed predominantly to climate variability. The IDPO variance (periods between ~9 and ~55 years) isolated from the $\delta^{18}O$ data of these five corals by SSA align reasonably well with each other back to 1650 (Figure 6). We argue that the reproducibility of the timing of the summed interdecadal and decadal components in the multi-coral $\delta^{18}O$ series demonstrates an environmental origin for this mode of $\delta^{18}O$ variability despite the variations in amplitude observed in some intervals. The five-coral Fiji-Tonga $\delta^{18}O$ series are from a region with a common climatic forcing related to the SPCZ and associated changes in SST and SSS (e.g., *Salinger et al.,* 1995; *Folland et al.,* 2002). *Folland et al.* [2002] identified this region of the southwest Pacific as a "center of action" for the PDO/IPO. Therefore we developed a Fiji-Tonga IDPO index from the five-coral $\delta^{18}O$ series we have generated.

To obtain the index we calculated an average of interdecadal-decadal variability from all 5 corals and the one-sigma error (see below and Figure 6) and term the result the Fiji-Tonga interdecadal-decadal Pacific Oscillation (F-T IDPO) index. The calculation of the index and its one-sigma standard error was performed as follows.

At each year t there are $n(t)$ records $x_1(t)$, $x_2(t)$…..$x_{n(t)}(t)$ available.

The index itself is computed as their mean:

$$\bar{x}(t) = \frac{1}{n(t)} \sum_{i=1}^{n(t)} x_i(t) \quad (1)$$

While it's standard error is computed as:

$$e(t) = \frac{\sigma(t)}{\sqrt{n(t)}} \quad (2)$$

where $\sigma(t)$ is unbiased estimate of the standard deviation of all records available for the year t, computed from:

$$\sigma^2(t) = \frac{1}{n(t)-1}\sum_{i=1}^{n(t)}\left(x_i(t) - \bar{x}(t)\right)^2 \quad (3)$$

The correlation coefficients of the IDPOs for all of the five cores are listed in Table 3. TM1 is least correlated with other cores. This could be due to its more southerly location between two different climatic zones [*Salinger et al.,* 1995] as previously mentioned and may mean that TM1 contains climatic information from both regions. However, we note that removing TM1 from the index does not modify our composite average significantly.

Potential chronological errors (1-2 years) in the $\delta^{18}O$ series may reduce the alignment (and R values), but chronological error is not likely to occur in all five cores in the same period of time and would not modify the five-coral composite greatly. Furthermore, ENSO-band (~3-8 years) variability in each coral $\delta^{18}O$ series was used to double-check the accuracy of the chronologies (not shown here), and the alignment of the ENSO band between the five corals supports the reliability of our chronologies back to at least 1715 A.D. We do note ENSO-band offsets between Fiji AB and Tonga TNI2 from 1715 to 1700 A.D. and from 1650-1660 A.D. (not shown), which probably are related to variations in interannual-scale chronology. One motivation for developing a Fiji-Tonga IDPO index from multiple coral cores is to minimize the potential

421 chronological errors and to reduce potential biological or diagenetic artifacts that can
422 affect individual $\delta^{18}O$ series, e.g., the variations in disequilibrium effect over time
423 between coral colonies [*Lough*, 2004; *Juillet-Leclerc et al.,* 2005; *Hendy et al., 2007*].
424 We expect the F-T IDPO index to be more representative of interdecadal-decadal
425 climatic variability in this region than any one of the five $\delta^{18}O$ series alone.

426 In dendroclimatology, the expressed population statistic (EPS) is used to determine
427 the number of records (N) required to produce an average (composite) with an
428 acceptable signal to noise ratio for the calculated mean interseries correlation
429 coefficient. *Wigley et al.* [1984] described the EPS. For dendroclimatology, the
430 acceptable EPS is often set subjectively to $\geq$0.85 [*Wigley et al.,* 1984*, Briffa* 1995].
431 *Delong et al.* [2007] described the application of the EPS approach to multiple
432 sub-annual resolution coral Sr/Ca records from New Caledonia. They found an
433 interseries correlation coefficient of 0.66 for annual averaged Sr/Ca data and concluded
434 that for their data an N=3 generates an EPS >0.85. For the more regionally spread
435 Fiji-Tonga corals, annual averaged $\delta^{18}O$ has a mean interseries correlation coefficient of
436 0.43 with all 5 corals, and 0.49 if we exclude core TM1 (Table 3). This indicates an
437 EPS of ~0.7 to 0.75. Using the EPS approach this would suggest that we need ~2 more
438 annual averaged $\delta^{18}O$ records from this region to generate an EPS > 0.85. Using our
439 approach described above we find an average unbiased estimate of the standard
440 deviation of the 5 coral $\delta^{18}O$ series is ±0.022‰ and that adding 2 more 200+ year $\delta^{18}O$
441 series to our index would reduce the error in the IDPO index by

(sqrt(7/5)-1)*100%=18%. Thus, although additional $\delta^{18}O$ series would improve the index, the current 5 coral composite index has significantly increased the signal to noise ratio for the interdecadal-decadal band and allows us evaluate this low-amplitude but important climate mode over time.

The coherence between this five-coral $\delta^{18}O$ IDPO composite and the SPI [*Folland et al.,* 2002] supports the reliability of this coral $\delta^{18}O$-based IDPO index and the method of SSA de-convolution to reconstruct interdecadal to decadal-scale climate changes in this region (Figure 7A). The correlation coefficient between the 3-year smoothed SPI and F-T IDPO is 0.39. Note that the SPI combines both ENSO and IDPO variances [*Folland et al.,* 2002]. The anti-phase correlation of the SPI (Figure 7A), but not of the IPO (Figure 7B) in the most recent 10 years may be due to the anomalous El Niño activity during this time period *(J. Salinger, personal communication*). The relatively low R-value may be caused by the ENSO component in the SPI that is excluded from the F-T IDPO index. Positive SPI values indicate a northeast displacement of SPCZ towards Apia (Samoa), creating cooler and saltier conditions in the study area (Fiji and Tonga) as the SSS front shifts to the west. This is in accord with times of more positive coral $\delta^{18}O$ in the F-T IDPO index. The consistency between the two indices, one oceanic and one atmospheric, confirms the climatic origin of the IDPO signal isolated in our five-coral composite index and the synchronous IDPO-scale oceanic and atmospheric changes in this area.

462 To evaluate the five-coral composite IDPO index further, we also compare it with
463 the IPO index of *Folland et al.* [2002], which is defined as the third Empirical
464 Orthogonal Function (EOF) of 13-year low-pass filtered Pacific SST over the period
465 1911-1995. The IPO is highly correlated with the PDO Index for the North Pacific, and
466 *Folland et al*. [2002] suggested that the IPO could be regarded as the Pacific-wide
467 manifestation of the PDO. The consistency between the F-T IDPO index and the IPO
468 (Figure 7B) indicates that the interdecadal to decadal-scale displacement of SPCZ
469 shown by F-T IDPO is also related to the IPO.

470 **4. 3 Time Evolution of the IDPO**

471 The interdecadal-decadal Pacific climate oscillation is relatively well recognized
472 after 1860 A.D. [e.g., *Mantua et al.,* 1997*; Power et al.,* 1999*; Hare and Mantua,* 2000;
473 *Folland et al.* 2002]. However, prior to this time, little is known about
474 interdecadal-decadal scale variability. Before 1860 A.D., our F-T IDPO index shows a
475 regular progression of positive and negative IPO phases (Table 4). The IDPO
476 oscillation appears to have been muted during ~1740 to mid-1750s and also during
477 mid-1680s to mid-1700s. These amplitude changes are observed in both of the coral
478 records that span these intervals (AB and TNI2) (Figure 6) and were abrupt with
479 pronounced IDPO variation before and after each period. This coral $\delta^{18}O$-based IDPO
480 index extends the existing instrumentally derived interdecadal-decadal oscillation
481 indices, e.g., the IPO and the PDO, back to 1650 A.D., providing a reliable reference for
482 the future study of lower frequency climatic oscillations.

The regularity of the F-T IDPO Index indicates that interdecadal-decadal variability in the SPCZ region has been relatively constant over the past 350 years with a mean frequency of ~20 years (variance peaks near 11 and 35yrs). This implies some degree of predictability of the IPO/PDO. Following the very strong El Niño of 1997-1998 both the F-T IDPO Index and the IPO index began a transition to a negative phase during which the central and eastern equatorial Pacific should be experiencing cooler then average conditions and the subtropics should be warmer than usual. Thus, based on the F-T IDPO regularity and assuming the continued anticorrelation between the F-T IDPO Index and the IPO/PDO, the Pacific should be in a La Niña-like mode (negative IPO phase) for next ~5-10 years then should transition back to a positive IPO phase and more El Niño-like conditions similar to the El Niño-dominated conditions that persisted during the last positive phase of the IPO from ~1976 to the late 1990s. The very strong (1982-1983 and 1997-1998) and prolonged (1990-1994) El Niño events that occurred during this period probably were enhanced by this positive IPO phase. Ignoring changes in the mean state of the Pacific, we suggest that future La Niña events in the next 5-10 years will be stronger due to the additive effects of the IPO phase while the strength of El Niño events will be weakened due to the phase of the IPO.

4. 4 F-T IDPO in-phase in SPCZ and WPWP

Comparison of the IDPO signal at Fiji and Tonga with the IDPO signal in two equatorial Pacific coral $\delta^{18}O$ records at Palmyra [*Cobb et al.,* 2001] and Maiana [*Urban*

504 *et al.,* 2000] yields a high anti-phase correlation (Figure 7C, R= -0.51 between Palmyra
505 and F-T IDPO; R= -0.41 between Maiana and F-T IDPO). This anti-phase correlation is
506 expected because Palmyra and Maiana are both located in an area where SST variability
507 is positively correlated to the IPO while SST in the Fiji and Tonga region is negatively
508 correlated with the IPO (Figure 1) [*Folland et al.,* 2002]. Palmyra (5.9°N, 162.1°W) is
509 located in the center of the tropical Pacific but outside of the WPWP and 1° north of the
510 Niño 3.4 region (shaded box in Figure 1), where ENSO has a larger amplitude than the
511 interdecadal-decadal oscillation [*Cobb et al.,* 2001]. If the coral $\delta^{18}O$
512 interdecadal-decadal changes at Palmyra are interpreted strictly as temperature (using a
513 range of published coral temperature-$\delta^{18}O$ regressions (0.17-0.23‰/°C) [e.g., *Epstein et*
514 *al.,* 1953*; Dunbar et al.,* 1994; *Gagan et al.,* 1994; *Wellington et al.,* 1996]), the total
515 range of the Palmyra interdecadal-decadal variability (~0.2‰) during 1886-1998
516 corresponds to ~1°C. This is the same order of magnitude as the interdecadal-decadal
517 variability derived from Niño 3.4 SST anomalies separated by SSA [*Kaplan et al.,*
518 1998]. This match suggests that the SST variability is the dominant factor affecting the
519 coral $\delta^{18}O$ values in Palmyra over interdecadal-decadal time scales.

520 In contrast to Palmyra, the $\delta^{18}O$ signal in Maiana records both SST and the
521 $\delta^{18}O_{seawater}$ (directly related to salinity) [*Urban et al.,* 2000]. Maiana (01°N, 173°E) is
522 located 25° west of Palmyra and is near the position of the salinity front on the eastern
523 edge of WPWP [*Donguy,* 1994; *Picaut et al.,* 1996]. Maiana $\delta^{18}O$ interdecadal-decadal
524 variability contains a similar pattern as that at Palmyra and in an opposite phase with

525 F-T IDPO. When a southwest shift of the SPCZ creates locally warmer and fresher
526 conditions (more negative $\delta^{18}O$ value) at Fiji and Tonga, it is accompanied by cooler
527 and saltier conditions at Maiana caused by less rainfall and/or a westward retreat of the
528 equatorial SSS front associated with the WPWP.

529 The eastward (westward) migration of the warm pool during the El Niño (La Niña)
530 phase of ENSO is well characterized by instrumental data [*Fu et al.,* 1986; *Picaut et al.,*
531 1996; *Delcroix and McPhaden,* 2002]. Due to the scarcity of long-term instrumental
532 data, the interdecadal-decadal scale displacement of the WPWP eastern salinity front is
533 less well understood. Recently, *Delcroix et al.* [2007] observed the presence of a
534 PDO-like SSS signal in the WPWP, the SPCZ and the Equatorial Cold Tongue during
535 1970-2003. Figure 8 shows the regression pattern (R values) of precipitation over the
536 interval from 1979 to 2000 [*Xie and Arkin* 1996] and SST over the interval from 1981 to
537 2000 [*Reynolds et al,* 2001] on the SPCZ position index (SPI) [*Folland et al.,* 2002].
538 Negative correlations (dashed contours) in Figure 8 reflect below average precipitation
539 and SST during positive SPI (and positive phase of the IPO) and positive correlations
540 (thin solid contours) indicate above average precipitation and SST during this positive
541 SPI and IPO phase. From Figure 8, it is clear that precipitation and SST regimes in the
542 Fiji-Tonga (SPCZ) area are reversed from those within the Maiana-Palmyra area of the
543 central equatorial Pacific. This observation agrees with the negative correlation between
544 the five-coral composite F-T IDPO index and Maiana-Palmyra, as discussed above.

545 The precipitation changes at Maiana and Palmyra during a positive phase of the

546 IPO are correlated to the same degree with the SPI (both sites are located between the
547 +0.4 and +0.6 contours in Figure 8). The same result was shown by *Delcroix et al.*
548 [2007; their Figure 5] which showed the regression of a 25-month filtered precipitation
549 product on the PDO index. In other words, the precipitation variance on
550 interdecadal-decadal time-scales appears to be comparable in these two places. If we
551 assume a near-linear relationship between $\delta^{18}O_{seawater}$, SSS and precipitation in this
552 region, the similar variability of Maiana and Palmyra rainfall on interdecadal-decadal
553 timescales is interesting since variability in coralline $\delta^{18}O$ at Maiana is due to both SST
554 and SSS while at Palmyra it is due mostly to SST. Presently, Maiana is located on the
555 WPWP eastern salinity front while Palmyra is in the center of the equatorial Pacific in a
556 region without a pronounced east-west SSS gradient and away from the WPWP. The
557 migration of the WPWP salinity front will modify SSS near Maiana, but not at Palmyra.
558 An implication of this is that the SSS changes at Maiana are mainly the result of zonal
559 and/or meridional advection, and not precipitation. This is the same conclusion reached
560 by *Delcroix and Picaut* [1998] and *Gouriou and Delcroix* [2002].

561 Displacements of the SPCZ salinity front can result from local variations in P-E
562 budget or zonal/vertical advection [*Gouriou and Delcroix*, 2002; *Delcroix et al.*, 2007].
563 In a positive phase of IPO, the westward shift of the SPCZ salinity front could result
564 from a local precipitation shortage or intensified South Equatorial Current. However,
565 when the precipitation deficit increases SSS during a positive IPO, lower SSTs will
566 reduce evaporation, which tend to offset the SSS increase caused by the precipitation

567 shortage. The opposite happens in a negative IPO phase. This increases our confidence
568 that zonal advection is the main contributor to the local SSS change in the SPCZ SSS
569 front region. *Gouriou and Delcroix* [2002] identified westward geostrophic surface
570 current velocity anomalies during El Niño years along 17ºS when the SPCZ salinity
571 front shifts westward, and eastward anomalies during La Niña years when the salinity
572 front shifts eastward. This strongly suggests an important role for surface zonal currents
573 in the east-west movement of the SPCZ salinity front on interannual time-scales. Due to
574 the lack of long-term instrumental record, we are not able to verify the strengths or
575 velocities of surface ocean current changes and their relationship with IPO, nor can we
576 conclude if the P-E budget or the zonal advection is the dominant factor controlling the
577 SPCZ salinity front shift. If there does exist a local westward surface current anomaly
578 from the cooler and saltier central Pacific Ocean in a positive IPO, it will push the
579 SPCZ salinity front westward and decrease local SST, which agrees with the IPO index
580 (derived from SST data [*Folland et al.*, 2002]) showing cooler-than-average conditions
581 in a positive IPO. The opposite will occur during negative IPOs, if there exists an
582 eastward surface current anomaly locally that will create warmer and fresher conditions
583 in SPCZ area.

584 Regardless of the exact mechanism, the opposite displacements of the eastern
585 WPWP and SPCZ salinity fronts are nearly synchronous on interdecadal-decadal
586 time-scales, with an average offset between interdecadal-decadal maxima-minima in
587 Maiana and corresponding minima-maxima in the F-T IDPO index of 0.8 years (stdev

588 =1.3 years)(see Figure 7). For Palmyra and the F-T IDPO index, the offset between
589 corresponding interdecadal-decadal minima and maxima, is 0.6 years (stdev = 1.1
590 years). The "propagating signal" hypothesis is one of the proposed mechanisms for
591 decadal-interdecadal variability (e.g., *Gu* and *Philander,* 1997; *Schneider et al*., 1999;
592 *Luo* and *Yamagata*, 2001). These authors argued that water masses subducted in the
593 eastern subtropical south Pacific would travel equator-ward and/or westward along the
594 pycnocline and then upwell along the equator once entrained in the swift equatorial
595 undercurrent. However, the synchronicity of the IDPOs of Maiana and Palmyra
596 (separated by 25º of longitude) indicates little or no time-lag for any IDPO signal
597 traveling along the equator. No time lag also appears between the IDPOs in the
598 equatorial Pacific and in the sub-tropical Fiji-Tonga region, thus neither region
599 (extratropical or tropical) appears to be leading. Any ocean or ocean-atmosphere
600 coupled models that simulate IPO variation should reflect this opposed yet simultaneous
601 process.

602 *Burgman et al.* [2008] described the atmospheric processes in the tropical and
603 subtropical Pacific during the 1990s IPO-PDO phase shift. This shift was observed in
604 our five-coral composite IDPO index and is the result of the correlation fields shown in
605 Figure 8. Their results suggested an increase in the east-west sea level pressure (SLP)
606 gradient on the equator and intensified Pacific atmospheric circulation during this
607 transition from positive IPO to negative IPO. The same response is also observed on
608 interannual time scales during the transition from El Niño (warm phase of ENSO) to La

609 Niña (cold phase). This could be the reason why we observe similar salinity front
610 movements on both interannual and interdecadal-decadal time scales on the eastern
611 edge of the WPWP and the SPCZ.

5. Conclusions

We have developed a coral $\delta^{18}O$ Fiji-Tonga Interdecadal-Decadal Pacific Oscillation (F-T IDPO) index based on annually averaged $\delta^{18}O$ time series from five corals collected in Fiji and Tonga (16°49'S-21°02'S; 179°14'E-174°43'W). The F-T IDPO index spans the period 1650-2004 A.D. and has been shown to closely track the IPO and SPI indices. Thus, this index effectively extends our knowledge of interdecadal-decadal ocean-climate variability for ~250 years prior to the instrumental record. The regularity of the F-T IDPO index indicates that interdecadal-decadal variability in the SPCZ region has been relatively constant over the past 350 years with a mean frequency of ~20 years (variance peaks near 11 and 35yrs). We note that during ~1740 to the mid-1750s and during the mid-1680s to the mid-1700s the amplitude of the interdecadal-decadal variability diminished sharply. We also observe an anti-correlation with coral $\delta^{18}O$ interdecadal-decadal components isolated from other equatorial Pacific coral records at Maiana and Palmyra. This suggests the simultaneous but opposite behavior between the SPCZ and western equatorial Pacific regions. By examining the pattern of precipitation response in Maiana and Palmyra during the last IPO positive phase, we conclude that at interdecadal-decadal time-scales, it is the displacement of the salinity front on the eastern edge of WPWP, instead of precipitation changes, that contributes to the SSS variance recorded by coralline $\delta^{18}O$ series at Maiana.

Our observations support the results of *Delcroix et al.* [2007] and suggests that the

633 anti-phase interdecadal-decadal variations between the equatorial Pacific and the SPCZ
634 region result from the opposing movements of the eastern WPWP and SPCZ salinity
635 fronts. In other words, the interdecadal-decadal eastward expansion (westward
636 contraction) of the WPWP salinity front occurs at the same time as the westward
637 (eastward) shift of the SPCZ salinity front. This anti-phase relationship between the
638 SPCZ and eastern WPWP is also observed on seasonal and ENSO time scales [*Gouriou*
639 and *Delcroix,* 2002]. The WPWP expands eastward during the South Hemisphere winter
640 when the SPCZ retracts; the opposite situation occurs in the South Hemisphere summer
641 when the SPCZ expands southeastward and eastern WPWP retreats westward. In the
642 warm phase of ENSO (El Niño), the eastern WPWP expands while SPCZ contracts and
643 in the cold phase (La Niña), the eastern WPWP retreats westward and SPCZ expands.
644 The synchronous changes of WPWP and SPCZ salinity fronts on interdecadal-decadal
645 time-scales could be evidence that atmospheric processes are involved as *Burgman et al.*
646 [2008] conclude. Finally, the regularity of the IPO/PDO over the last several centuries
647 suggests that La Niña events in the next 5-10 years will be stronger due to the additive
648 effects of the IPO phase while the strength of El Niño events will be weakened due to the
649 phase of the IPO.
650
651

651 **Acknowledgements**

652 For the Fiji component of this research we thank Mr. Saimone Tuilaucala (Director of
653 Fisheries) and Mr. Aisake Batibasaga (Principal Research Officer) of the Government of
654 Fiji, Ministry of Fisheries and Forests, for supporting this research program. We also
655 thank Jennifer Caselle, David Mucciarone, Tom Potts, Stefan Bagnato, Ove
656 Hoegh-Guldberg, and the J. M. Cousteau Resort in Savasavu (Fiji) for assistance with
657 field sampling. For the Tonga component of this work we gratefully acknowledge Mr.
658 'Ulunga Fa' Anunu (Acting Secretary of Fisheries, Ministry of Fisheries in Nuku'alofa)
659 and the Kingdom of Tonga for their support. We are also deeply indebted to the crew of
660 the R. S. V. Evohe (Captain Steve Kafka, Kelly McGrath, Allison Paulin, and Greg
661 Brosnan*) for their extraordinary assistance in coral core collection in Tonga during
662 November 2004. In Tonga Dr. Sandy Tudhope and Alexa Stolorow also contributed to
663 the collection effort. Earlier phases of this research was supported by NSF grant
664 OCE-0318296 and NOAA grant NA96GP0406 (to BKL), and NSF grant ATM-9619035
665 and NOAA grant NA96GP0470 (to GMW). This research is most recently supported by
666 NSF grant OCE-0318296 (to BKL) and OCE-0317941 (to A.K.). This is LDEO
667 contribution number 7147. *This paper is dedicated to the memory of Greg Brosnan
668 (Broz). Broz was instrumental in the success of our Tonga November 2004 drilling and
669 helped advance the state of underwater coral drilling. He died tragically in a glider
670 accident in New Zealand in January 2005.

671

References

Bagnato, S., B. K. Linsley, S. S. Howe, G. M. Wellington, and J. Salinger (2004), Evaluating the use of the massive coral *Diploastrea helipora* for paleoclimate reconstruction, *Paleoceanography*, *19*, PA1032, doi:10.1029/2003PA000935.

Briffa, K. R., (1995), Interpreting high resolution proxy-climate data- The example of dendroclimatology, in H. von Storch and A. Navarra *eds., Analysis of Climatic Variability*, Springer, Berlin, 77-94.

Boyer, T. P., Stephens, C., J. I. Antonov, M. E. Conkright, R. A. Locarnini, T. D. O'Brien, and H. E.Garcia, (2002) World Ocean Atlas 2001, Volume 2: Salinity. S. Levitus, Ed., NOAA Atlas NESDIS 50, U.S. Government Printing Office, Wash., D.C., 165 pp., CD-ROMs.

Burgman, R. J., A. C. Clement, C. M. Mitas, J. Chen, K. Esslinger (2008), Evidence for atmospheric variability over the Pacific on decadal timescales, *Geophys. Res. Lett.*, *35*, LOI1704, doi: 10.1029/2007GL31830.

Charles, C. D., D.E. Hunter, and R. G. Fairbanks (1997), Interaction between the ENSO and the Asian Monsoon in a coral record of tropical climate, *Science, 277*, 925-928.

Cobb, K. M., C. D. Charles, and D. E. Hunter (2001), A central tropical Pacific coral demonstrates Pacific, Indian, and Atlantic decadal climate connections, *Geophys. Res. Lett., 28,* No. 11, 2209-2212.

Cobb, K. M., C. D. Charles,; H. Cheng, and R. L. Edwards (2003), El Niño/Southern Oscillation and tropical Pacific climate during the last millennium, *Nature, 424*, 271-276.

Conkright, M.E., and T. P. Boyer (2002), World Ocean Atlas 2001: Objective Analyses, Data Statistics, and Figures, CD-ROM Documentation. National Oceanographic Data Center, Silver Spring, MD, 17 pp.

Crowley, T. J., T. M. Quinn, and W. T. Hyde, (1999), Validation of coral temperature calibrations, *Paleoceanography, 14*, 605-615.

Delcroix, T., and J. Picaut (1998), Zonal displacements of the western equatorial Pacific fresh pool, *J. Geophys. Res.*, *103*, 1087-1098.

Delcroix, T., and M. J. McPhaden (2002), Interannual sea surface salinity and

711 temperature changes in the western Pacific warm pool during 1992-2000, *J.*
712 *Geophys. Res.*, *107*(C12), 8002, doi: 10.1029/2001JC000862.
713
714 Delcroix, T., S. Cravatte, and M. J. McPhaden (2007), Decadal variations and trends in
715 tropical Pacific sea surface salinity since 1970, *J. Geophys. Res., 112*, C03012,
716 doi:10.1029/2006JC003801.
717
718 Delong, K. L., T. M. Quinn, F. W. Taylor, (2007) Reconstructing twentieth-century sea
719 surface temperature variability in the southwest Pacific: A replication study using
720 multiple coral Sr/Ca records from New Caledonia, *Paleoceanography*, *22*, PA4212,
721 doi:10.1029/2007PA001444.
722
723 Donguy, J-R. (1994), Surface and subsurface salinity in the tropical Pacific ocean:
724 Relations with climate, *Progr. Oceanogr.*, *34*, 45-78.
725
726 Dunbar, R. B., G. M. Wellington, M. W. Colgan, P. W. Glynn (1994), Eastern Pacific
727 sea surface temperature since 1600 A.D.: The $\delta^{18}O$ record or climate variability in
728 Galápagos corals, *Paleoceanography, 9* (2), 291-316.
729
730 Epstein, S., R. Buchsbaum, H. Lowenstam, and H.C. Urey (1953), Revised
731 carbonate-water isotopic temperature scale, *Geol. Soc. Am. Bull.*, *64*, 1315-1326.
732
733 Evans, M. N., A. Kaplan, and M. A. Cane (2000), Intercomparison of coral oxygen
734 isotope data and historical sea surface temperature (SST): Potential for coral-based
735 SST field reconstructions, *Paleoceanography, 15*, 551-564.
736
737 Fairbanks, R.G., M. N. Evans, J. L. Rubenstone, K. Broad, M.D. Moore, and C. D.
738 Charles (1997), Evaluating climate indices and their geochemical proxies
739 measured in corals, *Coral Reefs, 16*, 93-100,.
740
741 Folland, C. K., J. A. Renwick, M. J. Salinger, and A. B. Mullan (2002), Relative
742 influences of the Interdecadal Pacific Oscillation and ENSO on the South Pacific
743 Convergence Zone, *Geophys. Res. Lett.*, *29*. No.13, doi:10.1029/2001GL014201.
744
745 Fu, C. B., H. Diaz, J. Fletcher (1986), Characteristics of the response of sea surface
746 temperature in the central Pacific associated with the warm episodes of the
747 Southern Oscillation, *Mon. Wea. Rev.*, *114*, 1716-1738.
748
749 Gagan, M. K., A. R. Chivas, and P. J. Isdale (1994), High-resolution isotopic records
750 from corals using ocean temperature and mass-spawning chronometers, *Earth*
751 *Planet. Sci. Letts.*, *121*, no. 3/4, 549-558.

Gouriou, Y., and T. Delcroix (2002), Seasonal and ENSO variations of sea surface salinity and temperature in the South Pacific Convergence Zone during 1976–2000, *J. Geophys. Res.*, *107*(C12), 3185, doi:10.1029/2001JC000830.

Gu, D., and S. G. H. Philander (1997), Interdecadal climate fluctuations that depend on exchanges between the tropics and extratropics, *Science, 275*, 805–807.

Hare, S., and N. Mantua (2000), Empirical evidence for North Pacific regime shifts in 1977 and 1989, *Prog. Oceanography*, *47*, 103–146.

Hendy, E.J, M.K. Gagan, J.M. Lough, M. McCulloch, P.B. deMenocal, (2007) The impact of skeletal dissolution and secondary aragonite on trace element and isotopic climate proxies in *Porites* corals, *Paleoceanography*, *22*, PA4101, doi: 1029/2007PA001462.

Jones, P. D., K. R. Briffa, T. P. Barnett, and S.F.B. Tett (1998), High-resolution palaeoclimatic records for the last millennium: Interpretation, integration and comparison with General Circulation Model control-run temperatures, *The Holocene*, *8*, No.4, (17) 455-471.

Juillet-Leclerc, A., S. Reynaud, C. Rollion-Bard, J. P .Cuif, Y. Dauphin, D. Blamart, C. Ferrier-Pages, and D. Allemand (2005), The relative impact of vital effect and environmental factors on the coral skeleton oxygen isotope ratio. *Geophys. Res. Abstr.*, 7, 06587, 1607-7962/gra/ EGU05-A-06587.

Juillet-Leclerc, A., S. Thiria, P. Naveau, T. Delcroix, N. Le Bec, D. Blamart, and T. Corrège (2006), SPCZ migration and ENSO events during the 20th century as revealed by climate proxies from a Fiji coral, *Geophys. Res. Lett., 33*, L17710, doi:10.1029/2006GL025950.

Kaplan, A., M. Cane, Y. Kushnir, A. Clement, M. Blumenthal, and B. Rajagopalan (1998), Analyses of global sea surface temperature 1856-1991, *J. Geophys. Res., 103*, 18, 567-589.

LeGrande, A. N., and G. A. Schmidt (2006), Global gridded data set of the oxygen isotopic composition in seawater, *Geophys. Res. Lett. 33*, L12604, doi:10.1029/2006GL026011.

Linsley, B.K., R.B. Dunbar, G.M. Wellington, and D.A. Mucciarone, A coral based reconstruction of Intertropical Convergence Zone variability over Central America since 1707, *Journal of Geophysical Research*, *99*, no. C5, 9977-9994, 1994.

Linsley, B. K., R. G. Messier, and R. B. Dunbar (1999), Assessing between-colony oxygen isotope variability in the coral *Porites lobata* at Clipperton Atoll, *Coral Reefs, 18*(1), 13-27.

Linsley, B. K., G. M. Wellington, and D. P. Schrag, (2000), Decadal sea surface temperature variability in the subtropical Pacific from 1726 to 1997 A. D., *Science*, *290*, 1145-1148.

Linsley, B. K., G. M.Wellington, D. P. Schrag, L. Ren, M. J. Salinger, and A. W. Tudhope (2004), Geochemical evidence from corals for changes in the amplitude and spatial pattern of South Pacific interdecadal climate variability over the last 300 years, *Clim. Dym., 22*, 1-11.

Linsley, B. K., A. Kaplan, Y. Gouriou, J. Salinger, P. B. deMenocal, G. M. Wellington, and S. S. Howe (2006), Tracking the extent of the South Pacific Convergence Zone since the early 1600s, *Geochemistry Geophysics Geosystems, 7*, Q05003, doi:10.1029/2005GC001115.

Lough, J. M. (2004), A strategy to improve the contribution of coral data to high resolution, *Palaeogeography, Palaeoclimatology, Palaeoecology*, *204* (1-2), 115-143.

Luo, J-J and T. Yamagata (2001), Long-term El Nino-southern oscillation (ENSO)-like variation with special emphasis on the South Pacific, *J Geophys Res*, *105*, 22,211–22,227.

Mann, M. E., and J. Park (1994), Global-scale modes of surface temperature variability on interannual to century timescales, *J. Geophys. Res.*, *99* (D12), 25,819–25,834.

Mantua, N., S. Hare, Y. Zhang, J. Wallace, and R. Francis(1997), A Pacific interdecadal climate oscillation with impacts on salmon productions, *Bull. Amer. Meteor. Soc, 78*, 1069– 1079.

Minobe, S., T. Manabe, and A. Shouji (2002), Maximal Wavelet Filter and its application to didecadal oscillation over the Northern Hemisphere through the twentieth century, *J. Clim.*, *15* (9), 1064–1075.

Morimoto, M., O. Abe, H. Kayanne, N. Kurita, E. Matsumoto, and Y. Yoshida (2002), Salinity records for the 1997-98 El Niño from western Pacific corals, *Geophys. Res. Lett.*, *29* (11) 1540, doi:10.1029/2001.

Mueller, A., M. K., Gagan, and M. T. McCulloch (2001), Early marine diagenesis in corals and geochemical consequences for paleoceanographic reconstructions, *Geophys. Res. Lett.*, *28*, 4471-4474.

Pätzold, J. (1984), Growth rhythms recorded in stable isotopes and density bands in the reef coral *Porites lobata* (Cebu, Philippines), *Coral Reefs, 3*, No.2, 87-90.

Picaut, J., M. Ioualalen, C. Menkes, T. Delcroix, and M. McPhaden (1996), Mechanism of the zonal displacements of the Pacific Warm Pool: Implications for ENSO, *Science, 274*, 1486-1489.

Power, S., T. Casey, C. Folland, A. Coleman, and V. Metha (1999), Interdecadal modulation of the impact of ENSO on Australia, *Clim. Dym., 15*, 319–324.

Priess, K., T. Le Campion-Alsumard, S. Golubic, F. Gadel, B.A. Thomassin (2000), Fungi in corals: Black bands and density banding of *Porites lutea* and *P. lobata* skeleton, Marine Biology, *136*, 19-27.

Reynolds, R.W., and T. M. Smith (1994), Improved global sea surface temperature analyses using optimum interpolation, *J. Clim.*, *7* (6), 929-948.

Reynolds, R.W., N. A. Rayner, , T. M. Smith, , D. C. Stokes, and W. Wang (2001), An improved in-situ and satellite SST Analysis for climate, *J. Clim., 15*, 1609-1625.

Salinger, M. J., R. E. Basher, B. B. Fitzharris, J. E. Hay, P. D. Jones, J. P. Macvergh, and I. Schmidely-Leleu (1995), Climate trends in the South-west Pacific, *International Journal of Climatology, 15*(3), 285-302.

Schneider, N., S. Venzke, A. J. Miller, D. W. Pierce, T. Barnett, C. Deser, M. Latif (1999), Pacific thermocline thermocline bridge revisited, *Geophys Res Lett, 26,* 1329–1332.

Tudhope, A.W., G. B. Shimmield, C. P. Chilcott, M. Jebb, A. E. Fallick, and A.N. Dalgleish (1995), Recent changes in climate in the far western equatorial Pacific and their relationship to the Southern Oscillation: Oxygen isotope records from massive corals, Papua New Quinea, *Earth Planet. Sci. Lett., 136,* 575-590.

Urban, F. E., J. E. Cole, and J. T. Overpeck (2000), Influence of mean climate change on climate variability from a 155-year tropical Pacific coral record. *Nature*, *407*, 989-993.

875 Vautard, R., and M. Ghil (1989), Singular spectrum analysis in nonlinear dynamics,
876 with applications to Paleoclimatic time series, *Physica D*, *35*, 395-424.
877
878 Vautard, R., P. Yiou, and M. Ghil (1992), Singular-spectrum analysis: A toolkit for
879 short, noisy chaotic signals, *Physica D*, *58*, 95-126.
880
881 Wigley, T.M.L., K. R. Briffa, and P.D. Jones (1984), On the average value of correlated
882 time-series, with applications in dendroclimatology and hydrometeorology, *J.*
883 *Climate Appl. Meteorol., 23*(2) 201-213.
884
885 Wellington, G.M., R. B. Dunbar, and G. Merlen (1996), Calibration of stable oxygen
886 isotope signatures in Galapagos corals, *Paleoceanography 11*, 467-480.
887
888 Xie, P., and P. A. Arkin (1996), Analyses of global monthly precipitation using gauge
889 observations, satellite estimates and numerical model predictions, *J. Clim.*, *9*,
890 840-858.
891

Figure Captions:

Figure 1. Location of Fiji, Tonga, Maiana, Palmyra and the Nino 3.4 area (shaded box, 5°N-5°S, 120°-170°W) in relation to the South Pacific Convergence Zone salinity front near Fiji and Tonga, to the West Pacific Warm Pool salinity front near Maiana, and to the spatial pattern of the IPO [*Folland et al.,* 2002]. Background contours show the IPO as a covariance map of the 3rd EOF of low-pass filtered SST anomalies for 1911-1995. The contour interval is 0.04°C, negative contours are dashed, values < -0.12°C sparsely stippled, and those > +0.12°C densely stippled. The maximum rainfall axis of the SPCZ for 1958-1998 is also shown as a thick black line. Figure modified from *Folland et al.* [2002].

Figure 2: Study sites in Fiji and Tonga (black outlined circles) in relationship to annually-averaged sea surface salinity [data from *Boyer et al.,* 2002; *Conkright and Boyer,* 2002](contours in p.s.u). The SPCZ-related sea surface salinity front can be seen aligned northeast-southwest across the study area. Crosses (+) mark Apia, Samoa and Suva, Fiji. The difference in mean sea level pressure between this sites was used to define the SPCZ position Index (SPI)[*Folland et al.,* 2002].

Figure 3. The plots of TH1-H5 (top), TH1-H4 (middle) and TNI2-H1 (bottom) over the period of 1950-2004 illustrate the match of the annual cycles during El Niño events highlighted in brown and La Niña events highlighted in blue. The $\delta^{18}O$ data from TH1-H5 was spliced onto the top of TH1-H4 (with dead top) based on cross-dating with data from core TNI2 and by aligning El Niño and La Niña events (also see Supplemental Figure 1 for X-ray collage of the TH1 cores).

Figure 4. Annually averaged $\delta^{18}O$ data of the five corals from Fiji and Tonga with the twentieth century mean values removed. The black arrows show the 1982-1983 El Niño event. The $\delta^{18}O$ (‰) scale is the same for all five corals.

Figure 5. The relative contribution of SST and SSS changes to the coralline $\delta^{18}O$ variance in Fiji (top) and Tonga (bottom). The annual SST data back to 1900 is from the HadISST1. Note that there are data from two regions in Tonga (northern Tonga and southern Tonga). Regional SSS data back to 1976 is from *Gouriou and Delcroix* [2002]. The SST (°C) and $\delta^{18}O$ (‰) were plotted on a 0.2‰/°C scale and the SSS (p.s.u) and $\delta^{18}O$ (‰) were plotted on a 0.3‰/p.s.u. scale so that the relative contributions to $\delta^{18}O$ variability can be assessed (see text).

Figure 6. (Top) IDPO signals of the five coral $\delta^{18}O$ series from Fiji and Tonga (thin colored lines) filtered by SSA, from which the average F-T IDPO index was created (thick black line). Labeled arrows indicate the number of corals whose spectra were included in the average IDPO index during various time intervals. (Bottom) The F-T IDPO index shown with 1-sigma unbiased uncertainty envelop (see text).

Figure 7. A.) The alignment between the F-T IDPO index and SPI [*Folland et al.,*2002]. B.) The F-T IDPO index compared with the IPO Index [*Folland et al,* 2002]. The colored areas show the IPO phases revealed by the F-T IDPO index back to 1650 A.D. "+" indicates positive IPO phases and "-" indicates negative IPO phases. The IDPO phase changes are coherent with the instrumentally derived IPO and SPI indices. C.) F-T IDPO with two coral $\delta^{18}O$ series from the equatorial Pacific, both filtered by SSA to isolate the IDPO band. Note that the scale of the right-hand y-axis of the Maiana [*Urban et al.,* 2000] and Palmyra [*Cobb et al.,* 2001] $\delta^{18}O$ series have been reversed for easier comparison with the left-hand y-axis of the F-T IDPO index.

Figure 8. A.) Correlation of SPCZ position index (SPI) [*from Folland et al.,* 2002] against precipitation over the interval from 1979 to 2000 (R-values). Note that the SPI is based on the air pressure difference between Apia (Samoa) and Suva (Fiji). B.) Correlation of SPCZ position index (SPI) [from *Folland et al.,* 2002] against SST over interval from 1981 to 2000 (R-values). August to July annual means of precipitation and SST are computed from monthly analyses by *Xie* and *Arkin* [1996] and *Reynolds et al* [2001], respectively. The red and orange areas in both panels indicate regions with a positive correlation during this time of a positive phase of the IPO index when the equatorial central and eastern Pacific is warmer with enhanced rainfall and the SPCZ region is cooler and saltier. Note the location of our study sites at Fiji and Tonga and that of the coral-climate study sites at Maiana [*Urban et al.,* 2000] and Palmyra [*Cobb et al.,* 2001].

952

Core ID	Years	$\delta^{18}O$ Sampling	Water Depth	Location	Latitude and Longitude
1F	1997-1780	Millimeter-scale	10 m	Savusavu Bay, Fiji	16°49'S 179°14'E
AB	2001-1617	Millimeter-scale	10 m	Savusavu Bay, Fiji	16°49'S 179°14'E
TH1	2004-1794	Millimeter-scale and annually	1 m	Ha'afera, Tonga	19°56'S 174°43'W
TNI2	2004-1650	Millimeter-scale and annually	3.5 m	Nomuka Iki, Tonga	20°16'S 174°49'W
TM1	2004-1837	Millimeter-scale and annually	6 m	Malinoa, Tonga	21°02'S 175°08'W

953

954 Table 1. List of five *Porites lutea* coral cores used to develop the composite Interdecadal-Decadal
955 Pacific Oscillation (IDPO) index. Description of Fiji cores (designated 1F and AB) were given by
956 *Linsley et al.* [2004] and *Linsley et al.* [2006].

957

958

Core ID	Number of Samples Analyzed	Average Difference of Replicates	Average $\delta^{18}O$ value of NBS-19 standard analyzed daily. (n=number analyzed)
TH1-H4	522	0.036	-2.199±0.031 (n=135)
TH1-H5	192	0.039	
TM1	391	0.037	-2.195±0.030 (n=76)
TNI2-H1	889	0.056	-2.206±0.034 (n=152)
TNI2-H3	1306	0.047	-2.200±0.038 (n=218)

959

960

961 Table 2. The number of $\delta^{18}O$ measurement for each Tonga core studied here and the average
962 difference of replicate $\delta^{18}O$ measurement by core. The $\delta^{18}O$ results for the two Fiji cores have been
963 previously reported [*Linsley et al., 2004; 2006*].

964

965

Correlation Coefficient	Tonga, TNI2	Tonga, TM1	Fiji, 1F	Fiji, AB
Tonga, TH1	0.67	0.35	0.47	0.55
Tonga, TNI2		0.23	0.49	0.37
Tonga, TM1			0.24	0.53
Fiji, 1F				0.45

966 Table 3. The correlation coefficients (R values) between the Fiji and Tonga coral $\delta^{18}O$ IDPO indices.

967 The low correlation between TNI2 and AB may be due to their inconsistency during ~1750-1760
968 and ~1700-1720.

969

Time Interval	**IPO and IPDO phase (+) or (-)**
Present to ~2000	Negative (-)
~2000 to early 1980s	**Positive (+)**
early1980s to early 1970s	Negative (-)
early 1970s to early 1960s	**Positive (+)**
early 1960s to mid 1940s	Negative (-)
mid 1940s to early 1920s	**Positive (+)**
early 1920s to ~1910	Negative (-)
~1910 to late 1890s	**Positive (+)**
late 1890s to early 1890s	Negative (-)
~1890 to mid 1870s	**Positive (+)**
mid 1870s to mid 1840s	Negative (-)
mid 1840s to early 1830s	**Positive (+)**
early 1830s to early ~1800s	Negative (-)
early 1800s to early 1780s	**Positive (+)**
early 1780s to ~1770	Negative (-)
~1770 to early 1740s	**Positive (+)**
Early 1740s to 1720s	Negative (-)
1720s to 1680s	**Positive (+)**
1680s to late 1660s	Negative (-)
Late 1660s to mid 1650s	**Positive (+)**

970 Table 4: Positive and negative phases of the IPO and IDPO Index back to 1650 A.D. Note that during
971 a positive phase the equatorial central and eastern Pacific is warmer and the SPCZ region is cooler and
972 saltier. During a negative phase the equatorial central and eastern Pacific is cooler and the SPCZ
973 region is warmer and fresher.
974
975

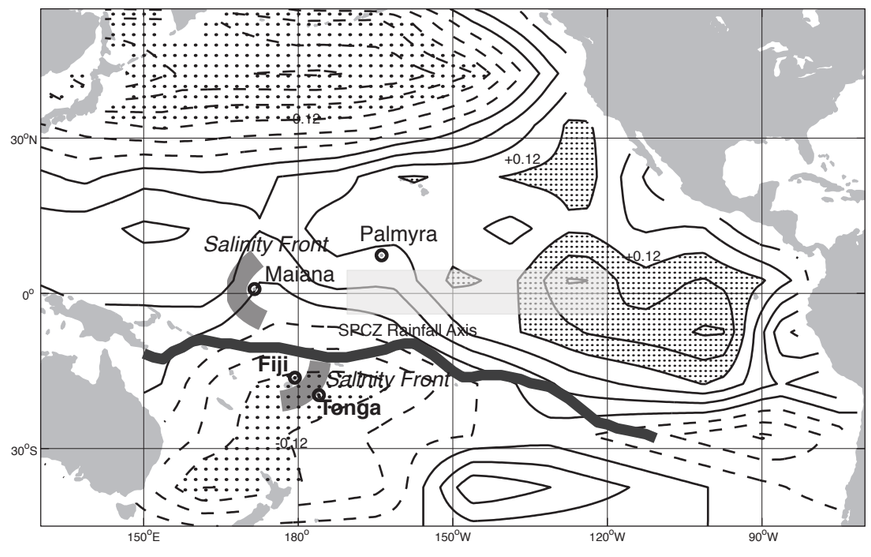
+0.12
+0.12
+0.12
+0.12
30°N
0°
30°S
Palmyra
Salinity Front
Malana
SRCZ Rainfall Axis
Fiji
Salinity Front
Tonga
150°E
180°
150°W
120°W
90°W

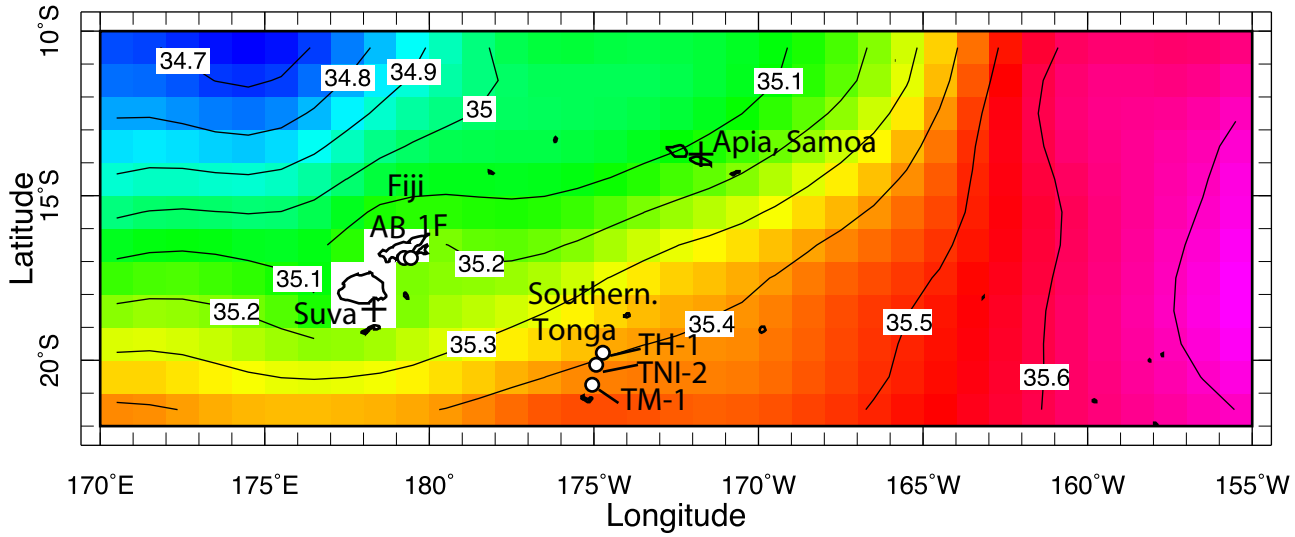
10°S
15°S
20°S
Latitude
34.7
34.8
34.9
35
35.1
35.2
35.3
35.4
35.5
35.6
Apia, Samoa
Fiji
AB_1F
Suva
Southern.
Tonga
TH-1
TNI-2
TM-1
170°E
175°E
180°
175°W
170°W
165°W
160°W
155°W
Longitude

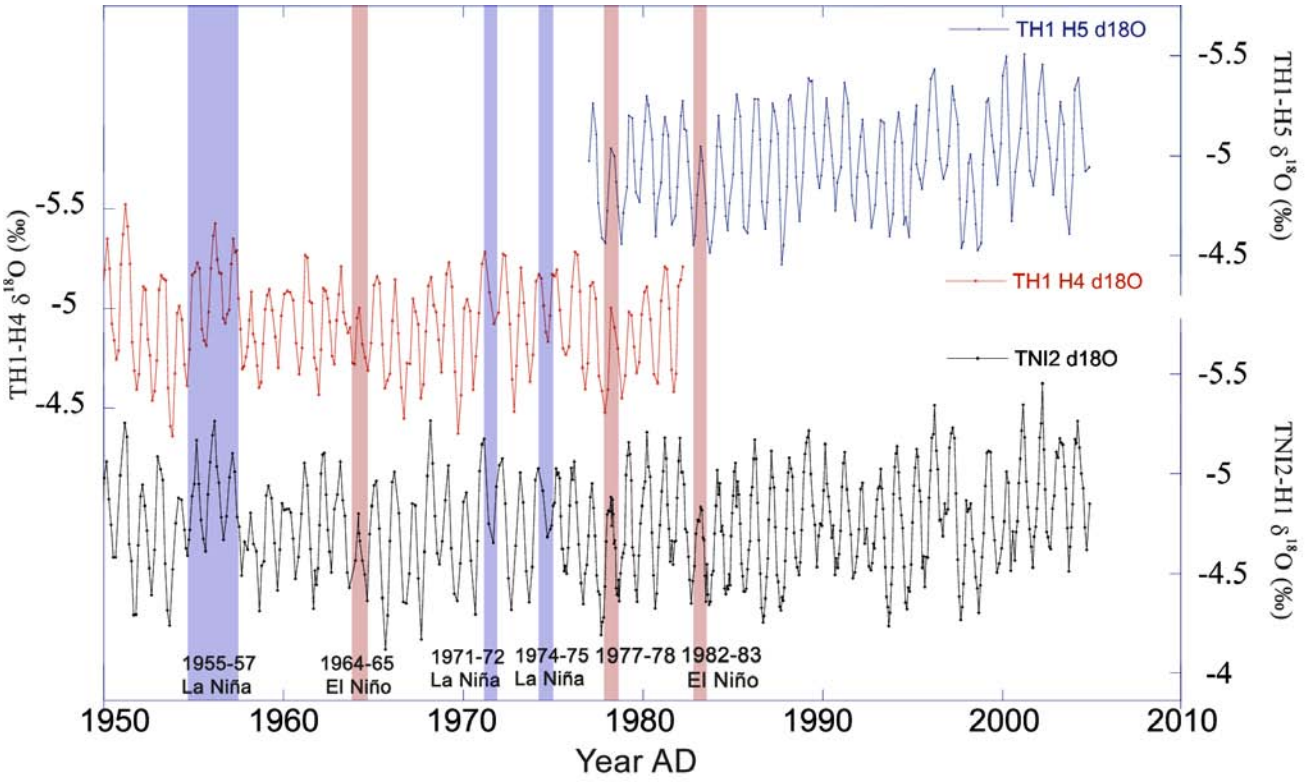
TH1 H5 d18O
TH1 H4 d18O
TNI2 d18O
TH1-H4 δ18O (‰)
TH1-H5 δ18O (‰)
TNI2-H1 δ18O (‰)
-5.5
-5
-4.5
-4
1955-57 La Niña
1964-65 El Niño
1971-72 La Niña
1974-75 La Niña
1977-78
1982-83 El Niño
1950
1960
1970
1980
1990
2000
2010
Year AD

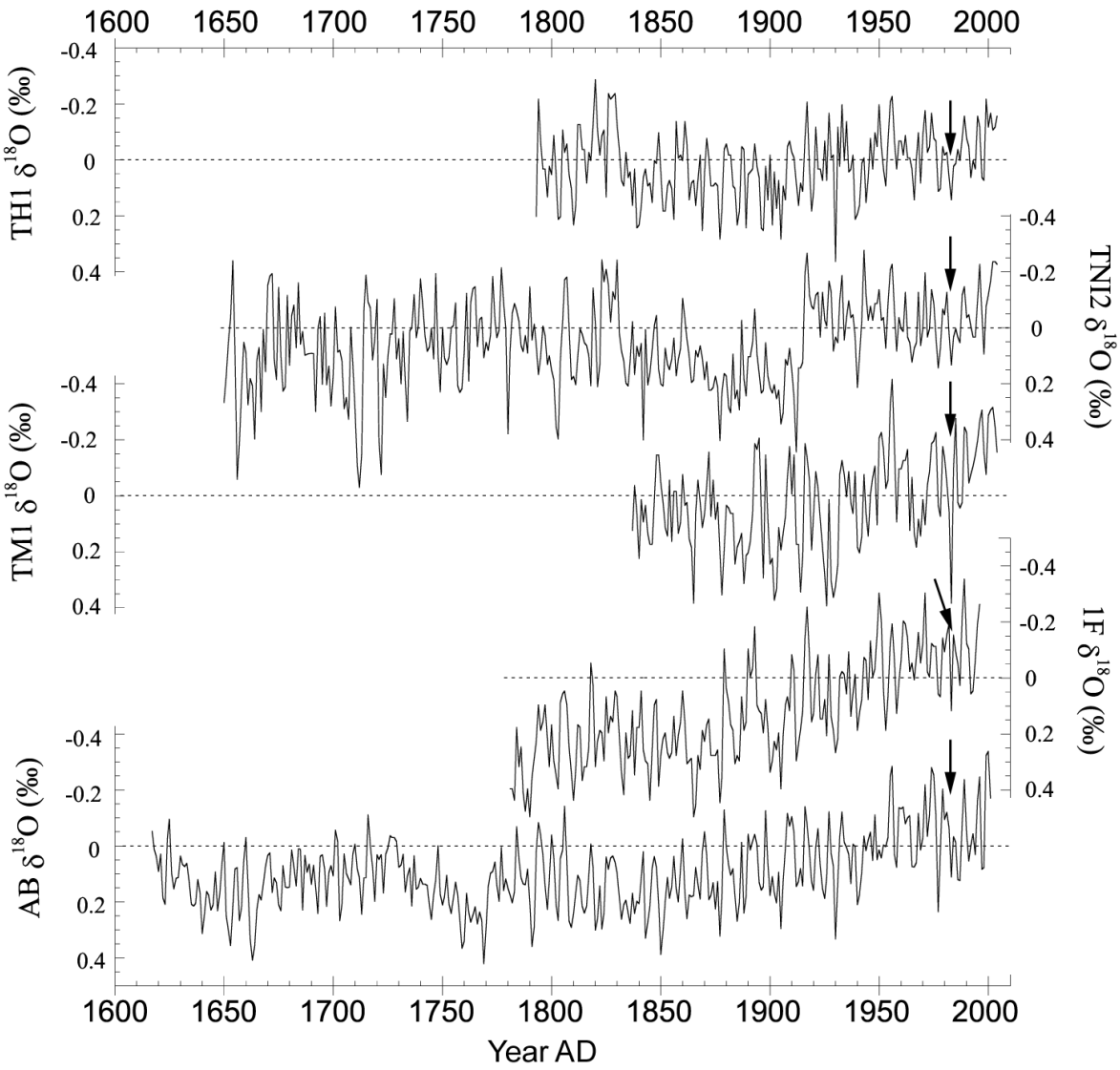
1600
1650
1700
1750
1800
1850
1900
1950
2000
TH1 δ18O (‰)
TNI2 δ18O (‰)
TM1 δ18O (‰)
1F δ18O (‰)
AB δ18O (‰)
-0.4
-0.2
0
0.2
0.4
Year AD

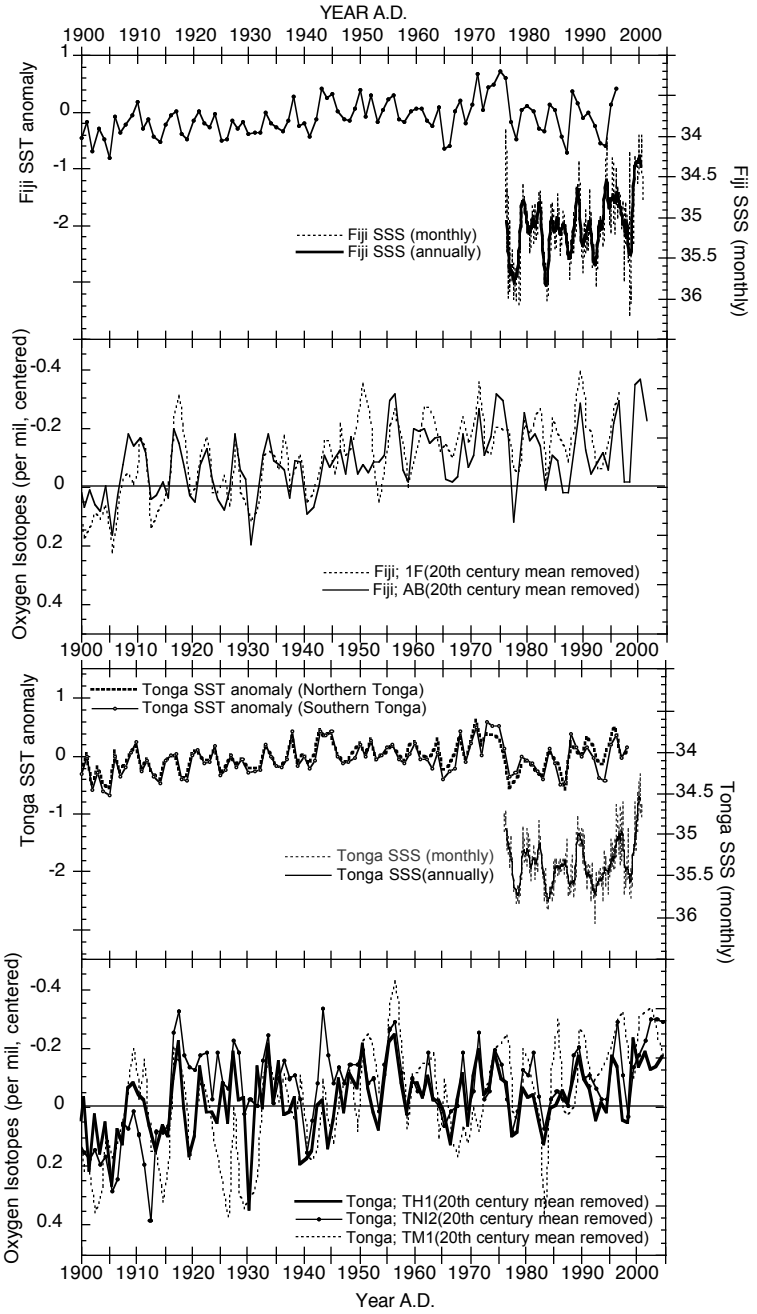
YEAR A.D.
1900 1910 1920 1930 1940 1950 1960 1970 1980 1990 2000
Fiji SST anomaly
Fiji SSS (monthly)
Fiji SSS (monthly)
Fiji SSS (annually)
Oxygen Isotopes (per mil, centered)
Fiji; 1F(20th century mean removed)
Fiji; AB(20th century mean removed)
Tonga SST anomaly (Northern Tonga)
Tonga SST anomaly (Southern Tonga)
Tonga SST anomaly
Tonga SSS (monthly)
Tonga SSS (monthly)
Tonga SSS(annually)
Oxygen Isotopes (per mil, centered)
Tonga; TH1(20th century mean removed)
Tonga; TNI2(20th century mean removed)
Tonga; TM1(20th century mean removed)
Year A.D.

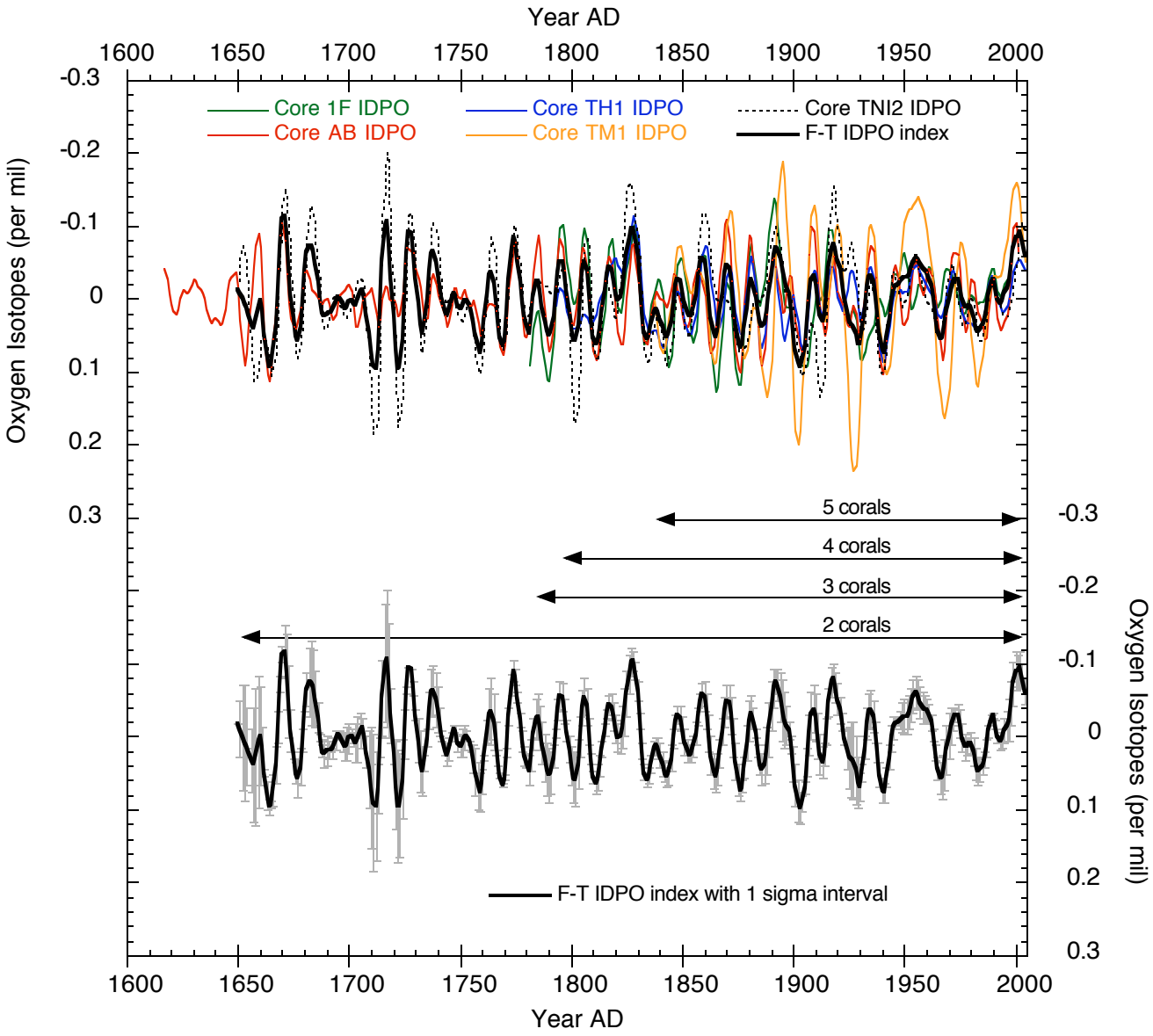
Year AD
1600
1650
1700
1750
1800
1850
1900
1950
2000
Oxygen Isotopes (per mil)
-0.3
-0.2
-0.1
0
0.1
0.2
0.3
Core 1F IDPO
Core AB IDPO
Core TH1 IDPO
Core TM1 IDPO
Core TNI2 IDPO
F-T IDPO index
5 corals
4 corals
3 corals
2 corals
F-T IDPO index with 1 sigma interval
Oxygen Isotopes (per mil)
Year AD

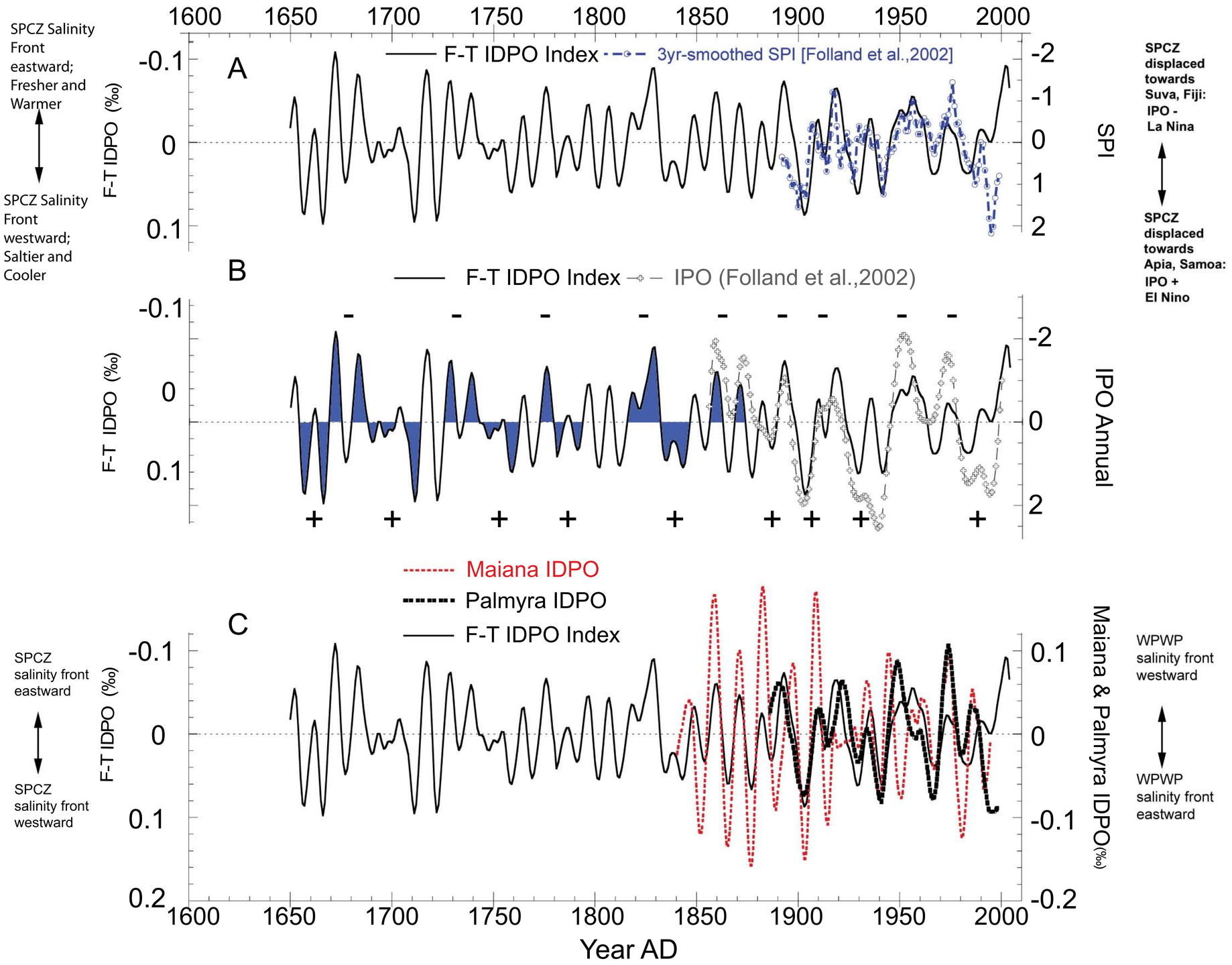
SPCZ Salinity Front eastward; Fresher and Warmer
SPCZ Salinity Front westward; Saltier and Cooler
1600
1650
1700
1750
1800
1850
1900
1950
2000
A
F-T IDPO Index
3yr-smoothed SPI [Folland et al.,2002]
F-T IDPO (‰)
-0.1
0
0.1
-2
-1
0
1
2
SPI
SPCZ displaced towards Suva, Fiji: IPO - La Nina
SPCZ displaced towards Apia, Samoa: IPO + El Nino
B
F-T IDPO Index
IPO (Folland et al.,2002)
IPO Annual
Maiana IDPO
Palmyra IDPO
F-T IDPO Index
C
SPCZ salinity front eastward
SPCZ salinity front westward
0.2
Maiana & Palmyra IDPO(‰)
WPWP salinity front westward
WPWP salinity front eastward
Year AD

A; SPCZ Position Index Correlated Against Precipitation

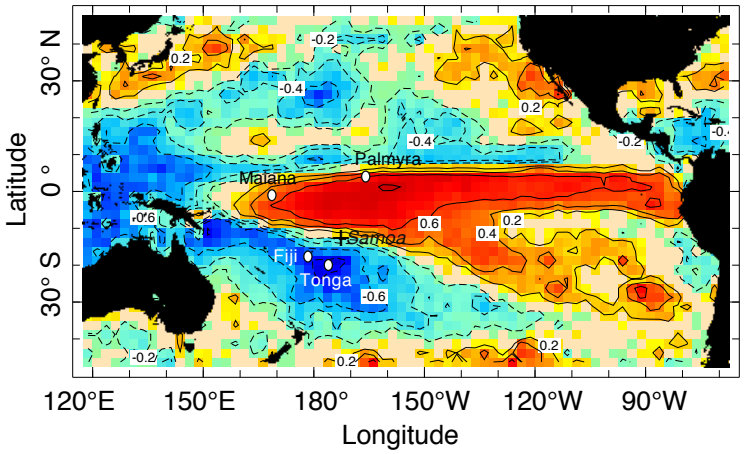

B; SPCZ Position Index Correlated Against SST